Electronic supplementary information (ESI)

Green synthesis and characterization of gold-based anisotropic nanostructures using bimetallic nanoparticles as seeds

Alfonso Nieto-Argüello[a], Alejandro Torres-Castro[b], Rafael Villaurrutia-Arenas[c], Juan J. Martínez-Sanmiguel[a], María Ujué González[d], José Miguel García-Martín[d] and Jorge L. Cholula-Díaz*[a]

[a] *School of Engineering and Sciences, Tecnologico de Monterrey, Av. Eugenio Garza Sada 2501, Monterrey 64849, N.L., Mexico.*

[b] *Faculty School of Mechanical and Electrical Engineering (FIME), Universidad Autónoma de Nuevo León (UANL), San Nicolás de los Garza 66451, N.L, Mexico.*

[c] *Thermofisher Scientific, Insurgentes Sur 863, Ciudad de México, 03810, Mexico*

[d] *Instituto de Micro y Nanotecnología, IMN-CNM, CSIC (CEI UAM+CSIC), Isaac Newton 8, Tres Cantos 28760, Spain.*

* Corresponding author: jorgeluis.cholula@tec.mx

Materials and methods

Chemicals

All chemicals and reagents were obtained from commercial sources and were used without further purification unless otherwise noted. Silver nitrate ($AgNO_3$; 99.70%) was purchased from J.T. Baker (Mexico City, Mexico), Sodium tetrachloroaurate (III) dihydrate ($NaAuCl_4{:}2H_2O$; 99%) was purchased from Sigma-Aldrich (St. Louis, M.O., U.S.A.), starch was purchased from CTR scientific (Monterrey, N.L., Mexico) and hydrogen peroxide (H_2O_2; 30.8%, Fermont, Monterrey, N.L., Mexico). Deionized (DI) water (σ = 18 MΩ cm) was used in the synthesis of bimetallic nanoparticle seeds and Au-ANs, as well as for all the procedures described below. All the glassware and stirring bars used in the synthetical procedure were kept in a 11.11% HCl solution for 24 h, then in a KOH/EtOH solution during the same period and rinsed with enough water before their use.

Synthesis of Ag/Au-NP seeds

The methodology used for the synthesis of colloidal noble bimetallic nanoparticle seeds was a modified method reported by Lomelí-Marroquín *et al.* [1]. First, an aqueous solution of 1% w/v starch was prepared and maintained under constant reflux and magnetic stirring for 30 min, subsequently the solution was centrifuged for 10 min at 3,500 rpm. The supernatant of the starch solution was added to DI water previously heated to 70 ± 1 ºC with a pH of 11.26 ± 0.12 reached by the addition of NaOH. For the synthesis of the Ag/Au-NP seeds with nominal atomic ratio 10:90 (Ag:Au), 50 µL of 25 mM $AgNO_3$ and 450 µL of 25 mM $NaAuCl_4$ were added to the mixture. The reaction was left in a water bath at 70 ºC for 2 h, and the resulting colloids were centrifugated twice for 60 min at 12,500 rpm. In each centrifugation step, the supernatant was discarded, and the remaining pellet was redispersed in 10 mL of water.

Synthesis of gold-based anisotropic nanostructures

The growth solution for the synthesis of Au-ANs consisted of Ag/Au-NP seed dispersion, 30.8% w/w H_2O_2, 1% w/v starch solution and water, according to the amounts specified in **Table S1**. In each case, the beginning of the reaction was considered after the addition of 300 µL of 25 mM $NaAuCl_4$ to the growth solution in increments of 30 µL every 2 s and under vigorous stirring. The resulting reaction mixtures were kept between 10 – 15 ºC up to 16 h.

Table S1 Various compositions of the growth solution in the synthesis of Au-based anisotropic nanostructures (Au-AN)

Sample	**Growth solution**				
	Seed dispersion / mL	H_2O / mL	1% w/v starch solution / µL	30.8% w/w H_2O_2 solution / µL	25 mM $NaAuCl_4$ / µL
Au-AN-1	6	4	0	30	300
Au-AN-2	6	3.5	500	30	300

Characterization of Ag/Au-NP seeds and Au-ANs

UV-vis spectroscopy

Localized surface plasmon resonance (LSPR) of the bimetallic nanoparticles (Ag/Au-NPs) seeds, as well as of the gold-based anisotropic nanostructures (Au-ANs) were characterized using a PerkinElmer 360 UV-vis spectrometer in the range between 300 and 1100 nm. For each measurement, the colloidal samples were diluted in a ratio 1:5 with water.

Transmission Electron Microscopy

The evaluation of size and morphology of the Ag/Au-NP seeds were carried out by Scanning Transmission Electron Microscopy (STEM) in a Talos F200X Thermo Scientific microscope

equipped with an extreme field emission gun (X-FEG) operated at 200 kV acceleration voltage and integrated with EDS system). For the Ag/Au-NP seeds a chemical compositional analysis was executed by using high-angle annular dark-field (HAADF)-STEM mode. The sample labelled as Au-AN-1 was further characterized by high resolution TEM imaging (HRTEM, FEI TITAN 80-300 equipped with a tungsten field emission gun operated at 300 kV accelerated voltage). The TEM equipment was integrated with a calibrated energy-dispersive X-ray spectroscopy (EDS) system (EDAX) for qualitative and quantitative elemental analysis. The samples for electron microscope imaging were prepared by drop casting on a carbon coated copper grid follow by air drying.

X-ray diffraction

The crystallinity of the synthesized nanostructures was determined by using a powder X-ray diffraction equipment (XRD, Rigaku Miniflex 600 diffractometer operating at a voltage of 40 kV, current of 15 mA and Cu-K_α radiation λ= 1.542 Å). The XRD samples were prepared by evaporating dropwise 8 mL of colloidal sample at 50 ºC on a cover glass. The XRD patterns were obtained in the diffraction angle (2θ) range of 25 – 100º at room temperature, using a step width of 0.05º (2θ) and scan speed of 1º/ min.

Fourier transformed Infrared spectroscopy

Fourier-transform infrared spectroscopy (FT-IR, Perkin Elmer 400 FT-IR/FT-NIR in attenuated total reflectance (ATR) mode) was used to prove the presence of a capping agent in each colloidal sample in the wavenumber range from 4000 to 400 cm^{-1}. For FT-IR spectroscopy, the dried samples for the XRD measurements were analysed.

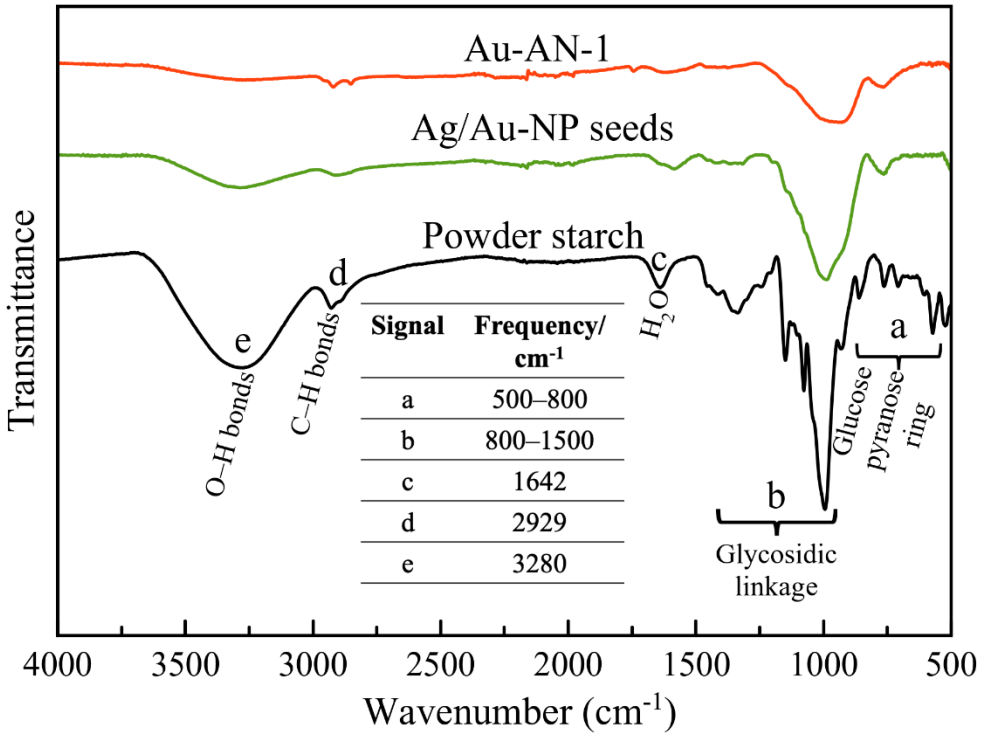

Fig. S1 FT-IR spectra of Ag/Au-NP seeds, Au-AN-1 and powder starch.

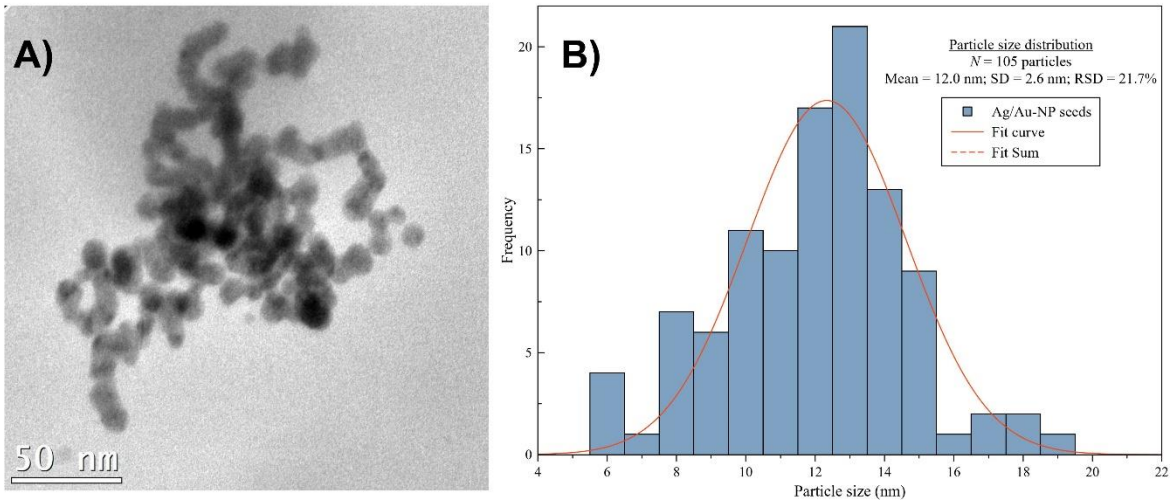

Fig. S2 Particle size characterization of Ag/Au-NP seeds. A) Representative STEM image. B) Histogram of the particle size distribution.

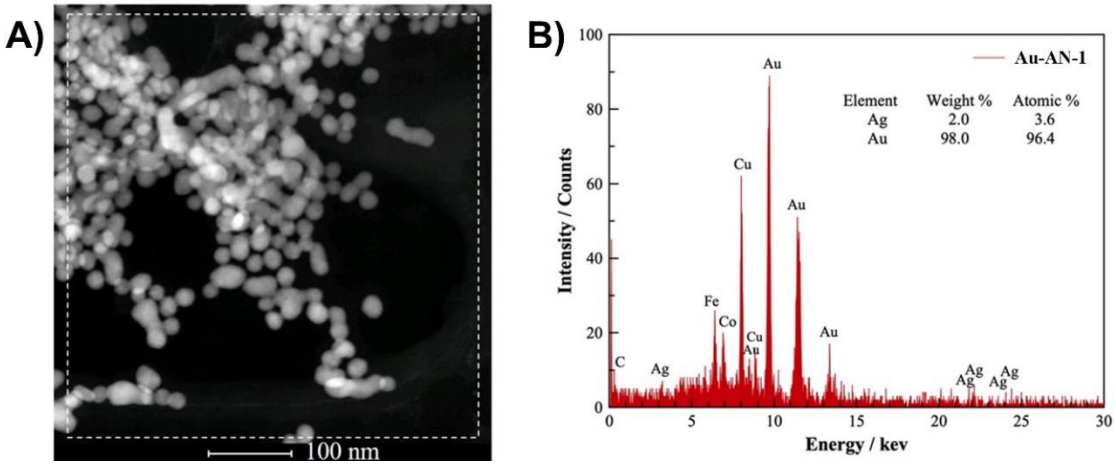

Fig. S3 Chemical composition analysis of the Au-AN-1 sample. A) STEM image and B) corresponding EDX analysis of the area enclosed. The presence of Cu is due to the TEM grid. The carbon (C) signal is due to the organic content (starch) in the sample. The iron (Fe) and cobalt (Co) signals are due to an unidentified source of contamination.

Table S2 Reported methods for the green synthesis of anisotropic gold nanostructures and their applications

Morphology and size	Reducing agent	Stabilizing or directing-growth agent	Application	Reference
Triangular plates and stars ~60 nm	Ascorbic acid	Gelatin	Radio-sensitizing effect of cancer cells	[2]
Triangular plates Edge length: 60-80 nm Thickness: ~8 nm	Liposomes	Liposomes	None	[3]
Stars Core:130-280 nm Branches: 15-55 nm	Ascorbic acid	Chitosan	Antibacterial effect	[4]
Triangular plates (35 nm) and various shapes	Portulaca oleracea Sterculia foetida	Portulaca oleracea Sterculia foetida	Cytotoxic effect against cancer cells	[5]
Nanoplates, nanorods, nanostars. Various sizes	H_2O_2[a]	None	Catalysis SERS	[6]
1 dimensional-chain network of spherical nanoparticles Various lengths	Tri-sodium citrate[b]	Tri-sodium citrate[b]	None	[7]
Triangular plates 150-200 nm	Cocoa extract[c]	Cocoa extract[c]	Photothermal therapy of cancer cells	[8]
Nanosheets Edge length: 50 μm Thickness: 20-50 nm	H_2O_2	Starch	Catalysis SERS	[9]

[a] First, spherical Au nanoparticle seeds were synthesized using NaBH4 and tri-sodium citrate as reducing and capping agents. Afterwards, the Au seeds were used to obtain the anisotropic nanostructures in the presence of H_2O_2.

[b] First, spherical Au nanoparticles were synthesized using tri-sodium citrate as reducing and stabilizing, followed by a dialysis process to obtain the anisotropic nanostructures.

[c] First, spherical Au nanoparticles were synthesized using cocoa extracts as reducing and stabilizing, followed by a sucrose-based density gradient centrifugation to obtain the anisotropic nanostructures.

References

[1] D. Lomelí-Marroquín, D. Medina Cruz, A. Nieto-Argüello, A. Vernet Crua, J. Chen, A. Torres-Castro, T. J. Webster and J. L. Cholula-Díaz, *Int. J. Nanomed*., 2019, 14, 2171–2190.

[2] R. P. Das, V. V. Gandhi, B. G. Singh and A. Kunwar, *New J. Chem*., 2021, 45, 13271–13279.

[3] J. Soto-Cruz, P. Conejo-Valverde, G. Sáenz-Arce, H. Dou and R.-C. O., *Langmuir*, 2021, 37, 3446–3455.

[4] P. Huynh, G. Nguyen, K. Tran, T. Ho, B. Duong, V. Lam and T. Ngo, *J. Nanomaterials*, 2021, 2021, 6650661.

[5] M. Firdhouse and P. Lalitha, *IET Nanobiotechnology*, 2020, 14, 224–229.

[6] M. A. Wall, S. Harmsen, S. Pal, L. Zhang, G. Arianna, J. R. Lombardi, C. M. Drainand M. F. Kircher, *Adv.Mater*., 2017, 29, 1605622.

[7] A. Dutta, A. Paul and A. Chattopadhyay, *RSC Adv*., 2016,6, 82138–82149.

[8] S. Fazal, A. Jayasree, S. Sasidharan, M. Koyakutty, S. V. Nair and D. Menon, ACS Appl. Mater. Interfaces, 2014, 6, 8080–8089.

[9] S. Nootchanat, C. Thammacharoen, B. Lohwongwatana and S. Ekgasit, *RSC Advances*, 2013, 3, 3707–3716.